Biochimica et Biophysica Acta 1850 (2015) 263–273

Contents lists available at ScienceDirect

Biochimica et Biophysica Acta

journal homepage: www.elsevier.com/locate/bbagen

Metabolic control analysis of the *Trypanosoma cruzi* peroxide detoxification pathway identifies tryparedoxin as a suitable drug target

Zabdi González-Chávez, Viridiana Olin-Sandoval [1], José Salud Rodíguez-Zavala, Rafael Moreno-Sánchez, Emma Saavedra *

Departamento de Bioquímica, Instituto Nacional de Cardiología Ignacio Chávez, México D.F. 14080, México

ARTICLE INFO

Article history:
Received 23 May 2014
Received in revised form 23 October 2014
Accepted 24 October 2014
Available online 30 October 2014

Keywords:
Trypanothione
Tryparedoxin
Trypanothione reductase
Peroxiredoxin
Flux control coefficient
Trypanosomatid

ABSTRACT

Background: The principal oxidative-stress defense in the human parasite *Trypanosoma cruzi* is the tryparedoxin-dependent peroxide detoxification pathway, constituted by trypanothione reductase (TryR), tryparedoxin (TXN), tryparedoxin peroxidase (TXNPx) and tryparedoxin-dependent glutathione peroxidase A (GPxA). Here, Metabolic Control Analysis (MCA) was applied to quantitatively prioritize drug target(s) within the pathway by identifying its flux-controlling enzymes.
Methods: The recombinant enzymes were kinetically characterized at physiological pH/temperature. Further, the pathway was *in vitro* reconstituted using enzyme activity ratios and fluxes similar to those observed in the parasites; then, enzyme and substrate titrations were performed to determine their degree of control on flux. Also, kinetic characterization of the whole pathway was performed.
Results: Analyses of the kinetic properties indicated that TXN is the less efficient pathway enzyme derived from its high Km_{app} for trypanothione and low *Vmax* values within the cell. MCA established that the TXN–TXNPx and TXN–GPxA redox pairs controlled by 90–100% the pathway flux, whereas 10% control was attained by TryR. The Km_{app} values of the complete pathway for substrates suggested that the pathway flux was determined by the peroxide availability, whereas at high peroxide concentrations, flux may be limited by NADPH.
Conclusion: These quantitative kinetic and metabolic analyses pointed out to TXN as a convenient drug target due to its low catalytic efficiency, high control on the flux of peroxide detoxification and role as provider of reducing equivalents to the two main peroxidases in the parasite.
General Significance: MCA studies provide rational and quantitative criteria to select enzymes for drug-target development.

1. Introduction

Trypanosoma cruzi is the causal agent of Chagas disease, which is endemic of Latin America, but it is now disseminated to non-endemic areas due to human emigration. The currently used drugs to treat this sickness are not commercially available and highly toxic. Then, more effective, less toxic and low cost alternative drugs are required [1,2]. This situation has prompted the quest for new therapeutic targets. The metabolic pathways that are unique and essential in the parasite and that significantly differ or are absent in the host have been investigated for therapeutic intervention. In this regard, the enzymes of the trypanothione-dependent antioxidant system in trypanosomatids [3–7] and in *T. cruzi* [8–10] have been proposed and studied for drug development.

In trypanosomatids, trypanothione ($T(SH)_2$) replaces glutathione (GSH) as the main antioxidant molecule. $T(SH)_2$ is a conjugate of two GSH molecules bound by a polyamine (usually spermidine), and it is synthesized by trypanothione synthetase (TryS). $T(SH)_2$ is the main reducing equivalents donor to the tryparedoxin-dependent hydroperoxide detoxification enzymatic machinery (Fig. 1). $T(SH)_2$ transfers electrons to the cytosolic dithiol protein tryparedoxin (TXN), which in turn deliver them to the tryparedoxin-dependent peroxiredoxin (TXNPx), the main peroxide detoxifying enzyme in the cytosol, or to other peroxidases such as the cytosolic non-selenium GSH-peroxidase-like tryparedoxin peroxidase (GPxA) [5–7]). Another membrane-embedded TXN isoform has been recently reported [11] whereas two isoforms of the peroxidases have also been found in mitochondria and endoplasmic reticulum of the parasite [4]. Further, TXNPx and GPxA from *Trypanosoma brucei* can reduce hydrogen peroxide, as well as

Abbreviations: C^{J}_{ai}, flux control coefficient; CumOOH, cumene hydroperoxide; GPxA, tryparedoxin-dependent glutathione peroxidase A; MCA, Metabolic Control Analysis; TryR, trypanothione reductase; TryS, trypanothione synthetase; $T(SH)_2$, trypanothione; TXN, tryparedoxin; TXNPx, tryparedoxin peroxidase; t-butOOH, tert-butyl hydroperoxide

* Corresponding author at: Departamento de Bioquímica, Instituto Nacional de Cardiología Ignacio Chávez, Juan Badiano No. 1 Col. Sección XVI, Tlalpan, México D.F. 14080, México. Tel.: +52 55 5573 2911x1298.
E-mail address: emma_saavedra2002@yahoo.com (E. Saavedra).
[1] Present address: Department of Biochemistry, University of Cambridge, Cambridge CB21GA, UK.

http://dx.doi.org/10.1016/j.bbagen.2014.10.029
0304-4165/

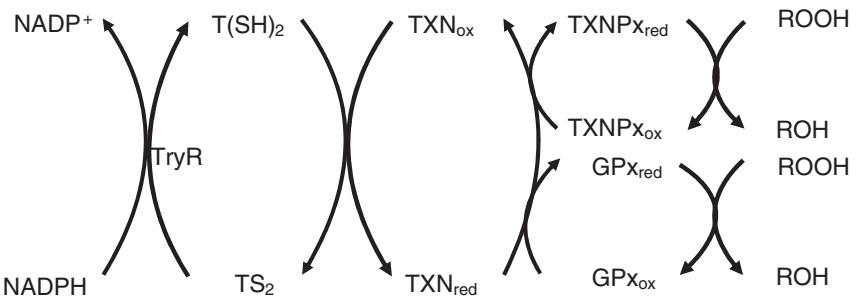

Fig. 1. Simplified scheme of the tryparedoxin-dependent hydroperoxide detoxification pathway in *T. cruzi*. For a complete description and discussion of this pathway see [4,6,8].

short-chain and alkyl/aryl peroxides with different affinities [12]; however, it is not known whether the enzymes from other trypanosomatids have the same characteristics. Finally, the oxidized trypanothione (TS_2) is reduced by trypanothione reductase (TryR) at the expense of NADPH oxidation.

By using knock-out or knock-down strategies performed mainly in *T. brucei* (since genetic engineering approaches are still under development in *T. cruzi*), it has been demonstrated that all enzymes of the TXN-dependent peroxide detoxification pathway, *i.e.* TryR, TXN and the peroxidases, are essential for parasite survival and oxidative stress management [13–15]. Therefore, all of these enzymes have been proposed as therapeutic targets for *T. brucei* and extrapolated to other trypanosomatids. However, it is now considered that besides genetic essentiality, subsequent levels of regulation/complexity such as enzyme activity (kinetome), pathway flux rates (fluxome) and metabolite concentrations (metabolome) should be included as criteria to select and prioritize drug targets in the trypanosomatid antioxidant system [6,16,17] and in general, in metabolic pathways of parasitic or pathogenic cells [18–20], to reach greater success treatment rates.

The fundamentals of Metabolic Control Analysis (MCA) [20–22] were here applied to identify the enzymes that mainly control the TXN-dependent hydroperoxide detoxification pathway in *T. cruzi* epimastigotes. This approach is used in the elucidation of the principal mechanisms of control and regulation of metabolic pathways. MCA allows the quantitative determination of the degree of control that a particular enzyme/transporter has on the pathway flux, namely flux control coefficient (C^J_{ai}), where *J* is flux and *ai* is the activity of any pathway enzyme/transporter. An enzyme/transporter with a C^J_{ai} value equal to the unity means that such step totally controls the pathway flux (a true traditional rate-limiting step). However, MCA experimental studies of different metabolic pathways have clearly established that the control of flux is generally shared in different degrees among several pathway steps, and therefore the existence of a unique rate-limiting step has been ruled out [20–22]. From the different experimental strategies that have been designed to determine the distribution of control of metabolic pathways (reviewed in [20]), enzyme titration in the *in vitro* reconstituted pathway was used in the present work to determine the individual flux control coefficients of the TXN-dependent peroxide detoxification pathway enzymes. Based on this quantitative analysis, the results indicated that the TXN–TXNPx and TXN–GPxA redox pairs exerted the major control of the pathway flux, with significantly lower control by TryR. Therefore, TXN could be the most convenient drug-target as it is located at the cross-road of the enzymatic detoxification machinery.

2. Methods

2.1. Parasite culture

Epimastigotes of *T. cruzi* Queretaro strain (DTU I) [23] were grown in liver infusion tryptose (LIT) medium [24] (DIFCO; Detroit, MI, USA), supplemented with 10% fetal bovine serum (PAA Laboratories; Pasching, Austria) and 25 μg ml^{-1} hemin and maintained at 26 °C. The cultures were initiated at a density of 4×10^6 parasites/ml and every 48 h they were diluted twofold with fresh LIT medium. Once the culture reached the late logarithmic phase (cellular density of ~25×10^6 parasites/ml), the parasites were collected for use.

2.2. Kinetic characterization of recombinant enzymes

Gene cloning, protein over-expression, purification and partial kinetic characterization of *T. cruzi* TryR, TXN, TXNPx and GPxA were previously described [25]. TryR activity was determined by monitoring the NADPH-dependent reduction of oxidized trypanothione (TS_2) as previously described [25]; $T(SH)_2$ was enzymatically prepared and purified as described elsewhere [26]. Product inhibition of TryR was determined by using 0.16 mM NADPH and 230 μM TS_2 (substrate) in the absence or presence of distinct concentrations of $T(SH)_2$ (product).

Enzymatic assays to determine the activities for TXN, TXNPx and GPxA were determined spectrophotometrically by monitoring the NADPH oxidation at 340 nm as described before [25], which were modified protocols from those originally described [27]. The assays were performed at pH 7.4 and 37 °C in a coupled system using oxidized trypanothione (TS_2) (previously reduced by TryR) and different hydroperoxides. Variations in the published protocols [25] are described below.

Kinetic parameters of GPxA with H_2O_2 and tert-butyl hydroperoxide (t-butOOH) were determined in assay buffer (40 mM Hepes pH 7.4, 1 mM EDTA) that contained 0.16 mM NADPH, 0.45 mM TS_2 or $T(SH)_2$, 0.5 μM TryR, 22 μM TXN, and the peroxides (0–1 mM H_2O_2 or 0–1 mM t-butOOH); after 3 min baseline stabilization, the reaction was started by adding 0.054–0.182 μM of GPxA.

TXNPx at concentrations lower than 1 μg/ml in the enzymatic assay was inactivated, as described before [28]. Therefore, to determine the Km_{app} values, the assay was carried out using a high TXNPx concentration and sub-saturating coupling enzymes and $T(SH)_2$ as reported before [29], with the inconvenience that the *Vmax*, and therefore, *kcat* values were underestimated. The reaction mixture contained assay buffer, 0.16 mM NADPH, 0.045 mM TS_2 or $T(SH)_2$, 0.01 μM TryR, 1 μM TXN, and 1 μM TXNPx (24 μg/ml), and the reaction was started by the addition of 0–400 μM H_2O_2. To determine the actual *Vmax* value of the recombinant enzyme (a mandatory requisite for the pathway reconstitution assays), TXNPx activity was assayed in the presence of 10% DMSO (to stabilize the enzyme), 0.16 mM NADPH, 0.45 mM TS_2/$T(SH)_2$, 0.5 μM TryR, 20 μM TXN, and 0.1 mM CumOOH and the reaction was started by adding 0.2–3.5 μg TXNPx.

For all activity assays, $T(SH)_2$ was previously calibrated by complete oxidation with H_2O_2 and further reduction with TryR and NADPH. To calibrate the peroxides, the tryparedoxin-dependent system coupled to NADPH oxidation was also used. Spurious activities in the absence of the specific enzyme or substrate were always subtracted. It was

ensured that the activity was linear with the amount of protein used (except for TXNPx in the absence of DMSO).

2.3. Enzyme activities in T. cruzi epimastigotes

Epimastigotes were cultured to the late logarithmic phase, and then harvested and washed, from which soluble cytosolic-enriched fractions were prepared as previously described [25]. Briefly, 500 million epimastigotes were harvested at 4500 *g* and washed twice with Phosphate Buffer-Saline (PBS; 137 mM NaCl, 2.7 mM KCl, 10 mM Na_2HPO_4, 2 mM KH_2PO_4, pH 7.4). The pellet was resuspended in 0.1 ml lysis buffer (20 mM Hepes pH 7.4, 1 mM EDTA, 0.15 mM KCl, 1 mM dithiothreitol, 1 mM phenylmethanesulphonyl fluoride) and lysed by three cycles of freezing/thawing. The cell lysate was centrifuged at 20,817 *g*, and the soluble fraction was collected for use. That this fraction was an enriched fraction of cytosol was demonstrated by determining the activity of pyruvate kinase, a marker of cytosol (Table S1 in supplementary material).

All the enzyme activities (*i.e.*, *Vmax*) were determined using saturating concentrations of the specific substrates and coupling enzymes. Strict controls were used to ensure that each particular enzyme activity was specifically determined: (i) the activity was initiated with the specific substrates (TS_2 for TryR) or ROOH (for TXN and the peroxidases), and the unspecific baseline activity previous to their addition was always subtracted; (ii) the activity was assayed only in the linear range of protein dependency; contaminating activities usually do not display this behavior (they do not show saturation); (iii) the order of addition of the components did not change the rate; (iv) no specific activity was attained in the absence of one enzyme (coupling or specific) component. Representative traces for each enzymatic assay are shown in supplementary material (Figs. S1, S2, and S3).

TryR activity in the cytosolic-enriched fractions was determined as previously described [25]. TXN activity was measured as described [25] with the following modification: the mixture containing assay buffer, 0.16 mM NADPH, 0.45 mM $T(SH)_2$, 0.5 μM TryR, 20 μM TXNPx and 0.1 mM CumOOH was pre-incubated for 3 min to monitor the spurious reaction of the peroxide with the assay components; then, the reaction was initiated by adding 0.1–0.6 mg/ml protein of parasite soluble cell fraction. TXNPx activity was determined in a saturating TryR/$T(SH)_2$/TXN assay containing assay buffer, 0.16 mM NADPH, 0.45 mM $T(SH)_2$, 0.5 μM TryR, 22 μM TXN and 0.1 mM CumOOH or t-butOOH and the reaction was initiated by the addition of 0.2–0.8 mg/ml protein of soluble cell fraction.

It was here determined that recombinant TXNPx and GPxA can use the same peroxides (Table 1). In the cytosolic-enriched fraction, GPxA activity was distinguished from that of TXNPx by using the GSH and glutathione reductase (GR) coupling system. The assay contained assay buffer, 0.16 mM NADPH, 10 mM GSH, 0.025 μM GR, 0.1 mM CumOOH and after 1 min baseline stabilization, the reaction was initiated by adding 0.4 mg protein soluble fraction/ml. Sub-saturating concentrations of GSH (10 mM) and CumOOH (0.1 mM; GPxA $Km_{app\ GSH}$ = 5 mM [30] and 0.1 mM CumOOH; Table 1) were used because GR is inhibited at high GSH concentration and higher peroxide concentration reacts non-enzymatically with GSH. To correct for these limitations, the recombinant GPxA activity was in parallel evaluated with both, the TryR/$T(SH)_2$/TXN and GSH/GR assays showing in the latter only 10% of the activity displayed with the former coupling system. Therefore, it was assumed that the GPxA activity in the cell determined with the GSH/GR assay was 10-fold underestimated (Table 1).

2.4. Hydroperoxide reduction flux in parasite soluble cytosolic-enriched fraction

The assay was carried out in assay buffer in the presence of 0.16 mM NADPH, 0.45 mM $T(SH)_2$ and 0.1 mM CumOOH (to saturate but not to inhibit TXNPx); the reaction was initiated by adding 0–2.5 mg of soluble cell protein and the NADPH oxidation due to TS_2 reduction was determined. The reduction rate of 30–100 μM H_2O_2 was also determined using the same assay. The unspecific NADPH oxidation in the absence of cell protein was always subtracted, whereas it was negligible in the absence of $T(SH)_2$.

2.5. Flux control coefficients

The reference reconstituted TXNPx pathway contained assay buffer to complete 0.5 ml, 0.16 mM NADPH, 0.45 mM $T(SH)_2$, 0.1 mM CumOOH and the following enzyme milliunits (nmol/min): 264 mU TryR, 88 mU TXN and 177 mU TXNPx, which are the enzyme activities determined in 1 mg of cytosolic-enriched fraction (Table 1). Higher $T(SH)_2$ concentrations in the physiological interval (up to 2 mM) were not used due to the high non-enzymatic rate of peroxide reduction (4 nmol/min with 1 mM $T(SH)_2$ and 80 μM CumOOH in the absence of enzymes; data not shown). When each enzyme was individually titrated, while keeping constant all the other variables in the system (partner enzymes and saturating substrates), the following activity intervals were screened: 0–1000 mU for TryR, 0–704 mU for TXN and

Table 1
Kinetic parameters of recombinant purified and soluble cell extract pathway enzymes.

Recombinant enzymes							*Enzymes in parasites*			
Enzyme	Substrate	*Km*	Inhibitor	*Vmax*	*Kcat*	*kcat/Km*	*Vmax*	*Km*	Inhibitor	*VmaxnKm*
TryR	TS_2	23 ± 6[a]	$T(SH)_2$	531 ± 137[a]	983[a]	4.3×10^{7}[a]	0.264 ± 0.15[a]			11.5[a]
	NADPH	9 ± 5[a]	IC_{50} = 2000 ± 300 [f]				0.195 ± 0.06			29.3
TXN	$T(SH)_2$	92 ± 20[a,b]		97 ± 20[a]	30 ± 6	$3.3 \pm 0.5 \times 10^{5}$	0.088 ± 0.014			0.95
TXNPx	TXN	0.6 ± 0.2		1.7 ± 0.5	7 ± 2	$1.3 \pm 0.7 \times 10^{7}$				295
				20 ± 5[c]	90 ± 4 [c]	1.5×10^{8}[c]				
	CumOOH	11 ± 4[a]	*Ki* = 888 ± 310	1.8 ± 0.5	7 ± 2	$6.5 \pm 0.5 \times 10^{5}$ 8.1×10^{6}[c]	0.179 ± 0.042	<8 (2)[g]	*Ki* > 400 (2)	16 22[d]
	t-butOOH	8 ± 3	*Ki* = 1446 ± 719	1.1 ± 0.2	4 ± 1	$5.6 \pm 2.3 \times 10^{5}$	0.177 ± 0.009[a]	<30 (2)[g]	*Ki* > 1000 (2)	22 6[d]
	H_2O_2	3.8 ± 2.9	*Ki* > 400	3.0 ± 2.9	12.3 ± 11.8	$6.5 \pm 9.2 \times 10^{6}$				47
GPx	TXN	2.3 ± 0.9[a]		15 ± 0.8	5.5 ± 0.3	$2.6 \pm 1.0 \times 10^{6}$	0.007 (2) 0.07[e]			3 30[e]
	CumOOH	106 ± 16[a]	*Ki* > 1000	31 ± 9	11 ± 3	$1.1 \pm 0.5 \times 10^{5}$				0.066 0.66[e]
	t-butOOH	442 ± 20	*Ki* > 800	22 ± 10	8 ± 4	$1.9 \pm 0.9 \times 10^{4}$				0.015 0.15[e]
	H_2O_2	313 (2)	*Ki* > 1000	29 (2)	11 (2)	3.3×10^{4} (2)				0.022 0.22[e]

Km and *Ki* values in μM; *Vmax* in μmol/min* mg protein; *kcat* in s^{-1}; *kcat/Km* in M^{-1} s^{-1}; *Vmax/Km* in ml/min* mg cell protein. For *Km* determination of recombinant enzymes, the rates were determined at saturating concentrations of co-substrates and coupling enzymes, except for TXNPx without DMSO (see Section 2) therefore, for this enzyme the *Km* and *Vmax* values indicated are apparent except for those indicated with [C]. The *Vmax* values in soluble cytosolic-enriched fractions were determined at saturating concentrations of all substrates and coupling enzymes. [a] Values reported in [25]. [b] see Fig. S5 for kinetic behavior. [c] values obtained in the TXNPx assay stabilized with 10% DMSO and using saturating TXN and CumOOH concentrations. [d] Values obtained using the *Km* determined in the cell fraction. [e] Value recalculated assuming that the GPxA *Vmax* was underestimated by 10 fold in the GSH/GR assay. [f] see kinetic behavior in Fig. S4. [g] Minimum values in which changes in activity were observed. Values are means ± SD of individual fittings made with at least three independent protein purifications or biological samples, except where indicated.

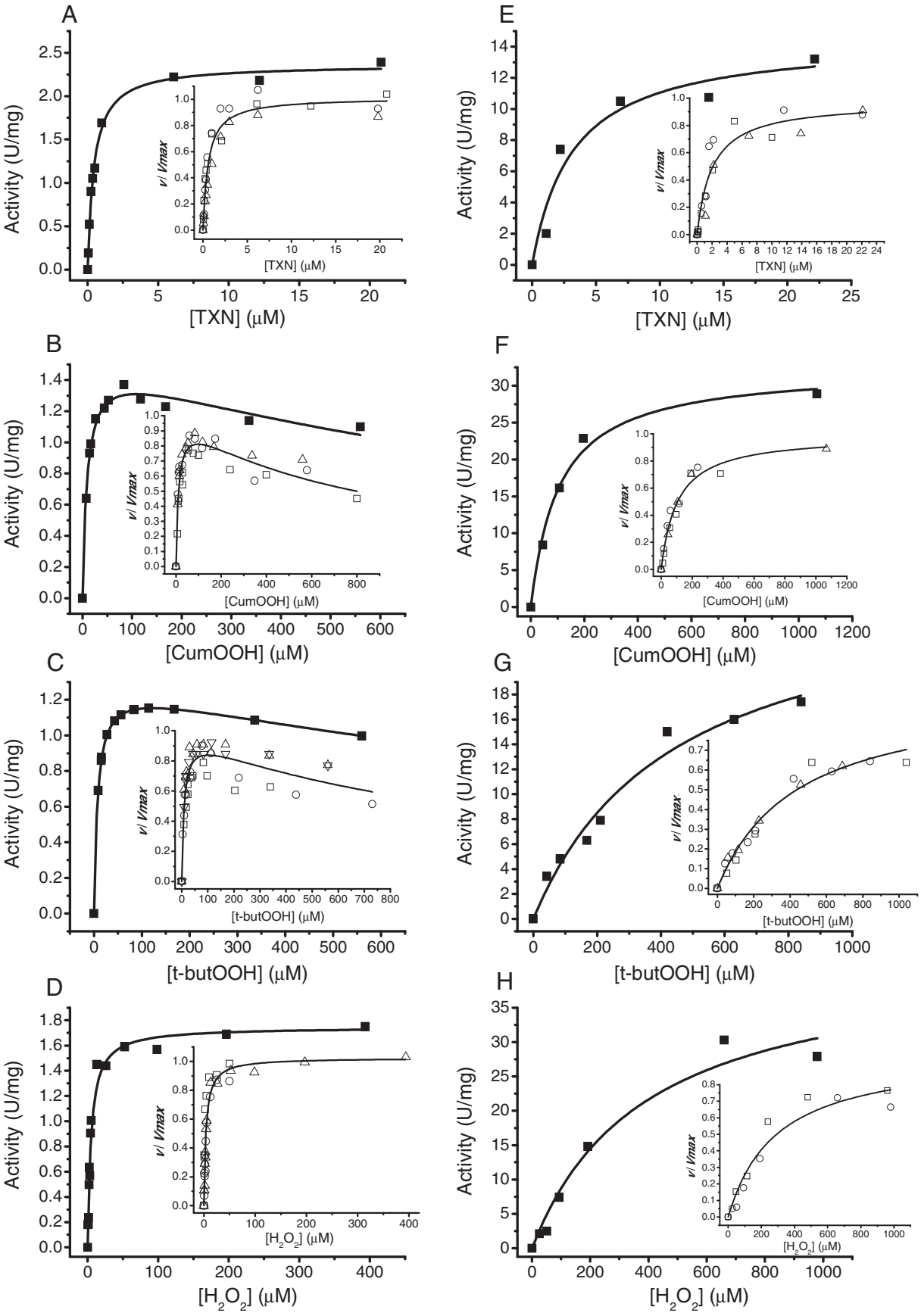
A
Activity (U/mg)
[TXN] (μM)
v/ Vmax
[TXN] (μM)
E
Activity (U/mg)
[TXN] (μM)
v/ Vmax
[TXN] (μM)
B
Activity (U/mg)
[CumOOH] (μM)
v/ Vmax
[CumOOH] (μM)
F
Activity (U/mg)
[CumOOH] (μM)
v/ Vmax
[CumOOH] (μM)
C
Activity (U/mg)
[t-butOOH] (μM)
v/ Vmax
[t-butOOH] (μM)
G
Acivity (U/mg)
[t-butOOH] (μM)
v/ Vmax
[t-butOOH] (μM)
D
Activity (U/mg)
[H2O2] (μM)
v/ Vmax
[H2O2] (μM)
H
Activity (U/mg)
[H2O2] (μM)
v/ Vmax
[H2O2] (μM)

0–1400 mU TXNPx; the pathway flux (NADPH oxidation) was in parallel determined. Just before each titration experiment, the activities of all the enzymes were verified to adjust for variations in the activity of the purified protein batches. The pathway was also reconstituted using 70 mU GPxA instead of TXNPx in the reference reconstituted pathway. The variations of activities were 0–528 mU for TryR, 0–176 mU for TXN and 0–140 mU for GPxA. To explore the effect of molecular crowding, the reference reconstituted pathway assay was performed in the presence of up to 50% PEG 8000 and 30% DMSO.

2.6. Affinities of the reconstituted pathway to substrates

Using the reference reconstituted system with TXNPx, the affinities of the whole pathway for the three substrates were determined. Ranges of variation were 0–0.19 mM for NADPH, 0–0.6 mM for $T(SH)_2$, and 0–0.3 mM for CumOOH or 0–0.4 mM for H_2O_2. When one substrate was varied, the other two were kept constant at the following concentrations: 0.16 mM NADPH, 0.45 mM $T(SH)_2$ and 0.1 mM CumOOH.

3. Results

3.1. Kinetic characterization of the enzymes involved in the TXN-dependent hydroperoxide reduction

Kinetic parameters of TryR, TXN, TXNPx and GPxA were here extended from those partially reported by our group [25]. The parameters were all determined in the same assay buffer at pH 7.4 and 37 °C, which resembled the physiological conditions of cytosolic pH [31] and temperature of the host for the *T. cruzi* bloodstream trypomastigotes, the medically important infective form. Thus, the determination of the kinetic parameters of the recombinant enzymes (Table 1) provided the background information required for pathway reconstitution at physiological pH and temperature. This allowed establishing appropriate and physiologically meaningful kinetic comparisons, which is not possible when the kinetic parameters are determined under different physicochemical conditions (*i.e.* the optimal assay conditions for each enzyme are not equal).

The *Vmax* and *Km* of recombinant and native TryR were similar to values reported by other groups [32]. The activity of recombinant TryR was evaluated in the presence of its product $T(SH)_2$ (Fig. S4). At concentrations lower than 0.7 mM the activity was not affected whereas at a higher concentration it was inhibited, reaching 50% inhibition at 2.0 ± 0.3 mM of $T(SH)_2$. Substrate-product competition or alteration of the reaction equilibrium by the high product concentrations used may be involved in this effect, although further studies are necessary to elucidate the inhibition mechanism. As the intracellular $T(SH)_2$ concentrations for several parasite stages are 0.3–2.2 mM [5,6,8,25], TryR activity may be partially inhibited depending on the $T(SH)_2$ concentration and type of inhibition.

TXN displayed a hyperbolic behavior with $T(SH)_2$ (Fig. S5) and, among the four enzymes, also showed the highest *Km* value for its substrate and the lowest catalytic potential (*kcat*/*Km*) for the thiol metabolite (Table 1).

TXNPx and GPxA showed hyperbolic kinetics with TXN (Fig. 2A and E) and their Km_{app} and *Km* values, respectively, were similar to those reported earlier, which were determined at pH 7.6 and 8.0, respectively [29,33]. TXNPx exhibited lower Km_{app} values for the evaluated peroxides (Fig. 2B–D) than GPxA (Fig. 2F–H) (Table 1), because the latter probably prefers long-chain fatty acid hydroperoxides, as has been reported for the *T. brucei* enzymes [12]. Although the *Vmax* of recombinant TXNPx was underestimated, and so its $kcat/Km_{app}$ value, TXNPx was nevertheless more efficient than GPxA in detoxifying H_2O_2, a physiologically important peroxide. Under saturated assay conditions, TXNPx is one order of magnitude more efficient than GPxA.

A previous report [28] described that TXNPx was inhibited by hydroperoxides, although no information about the conditions used or the degree of inhibition was disclosed. This enzyme was indeed inhibited by the short-chain hydroperoxides but not by H_2O_2 (Fig. 2B–D) with *Ki* values in the mM interval (Table 1). It was found that CumOOH inactivated whereas t-butOOH inhibited the enzyme: TXNPx pre-incubated for 2 min with 800 μM CumOOH at 37 °C lost 50% activity (determined by diluting and measuring the activity with 80 μM CumOOH); such inactivation was not observed by pre-incubating with t-butOOH (data not shown). In contrast, GPxA was not inhibited by any of the tested peroxides (Fig. 2F–H).

It was previously reported that GPxA was not able to reduce H_2O_2 when using the GSH/GR coupling system [30]. However, by changing to the TryR/$T(SH)_2$/TXN coupling system, GPxA could readily reduce H_2O_2, although with higher *Km* and lower catalytic potential than TXNPx (Fig. 2D–H; Table 1). A comparison of the GPxA activity in the two coupling assays was done using CumOOH. GPxA activity coupled to the GSH/GR system showed only 5–10% of the *Vmax* value (1.5 U/mg) and 30 times higher *Km* (3.1 mM) (Fig. S6) compared to the values attained with the TryR/$T(SH)_2$/TXN coupling system (Fig. 2F; Table 1). Therefore, the GSH/GR system is less efficient for GPxA activity determination.

Due to TXNPx instability induced by dilution in the enzymatic assay, its kinetic characterization (Table 1) was carried out at high TXNPx concentration and non-saturating concentrations of co-substrates and coupling enzymes, in which a stable linear initial-rate for at least 10 min was obtained. However, in the saturating assay with low TXNPx concentration *plus* the presence of 10% DMSO, the enzyme stability was improved for a short period of at least 10 s in which an initial-rate was reliably determined; in the presence of DMSO, the TXNPx activity showed a linear-dependency on the amount of enzyme used and a *Vmax* value of 20 ± 5 U/mg protein was obtained (Table 1).

3.2. Kinetic characterization of the enzymes in parasite soluble cytosolic-enriched fractions

To determine physiologically meaningful C^{l}_{ai} values by *in vitro* reconstitution of a cellular metabolic pathway, a similar ratio of the enzyme activities found in the parasites should be used; hence the *Vmax* values in the epimastigotes were thoroughly examined (Table 1). A soluble cell fraction was chosen as representative of a cytosol-enriched cell fraction since the main activity of the $T(SH)_2$ pathway enzymes is primarily located in the cytosol [8,33,34]. The presence of anti-oxidant enzyme isoforms proceeding from organelles is expected to be low because most of the cellular protein resides in the cytosol (>50%), with <5% derived from glycosomes in *T. brucei* [35]. Furthermore, strict controls in the kinetic assays were applied (see Section 2 for details) to ensure the determination of specific activities (see also Figs. S1, S2 and S3). Samples from trypomastigotes could not be used due to the large number of parasites necessary to obtain sufficient protein for enzymatic

Fig. 2. Kinetic characterization of recombinant TXNPx (A–D) and GPxA (E–H) at physiological pH and temperature. Representative plots of the kinetic characterization of both peroxidases with different substrates. The insets show the global fitting for titrations made with different independent protein batches (n = 2–4), which are indicated with different symbols; the *Km* values derived from these global fittings were similar to those shown in Table 1, which were calculated from each individual experiment and averaged. The data were fitted to the Michaelis–Menten equation using the Origin 8 software, except for B and C which were adjusted to the MM + substrate inhibition equation:

$$v = \frac{Vmax * S}{(Km + S) * \left(1 + \frac{S}{Ki}\right)}$$

determinations.

In the parasites, TryR was the enzyme with the highest *Vmax* in the TXN-dependent peroxide detoxification system (Table 1). Regarding TXN, we previously reported a high TXN activity (0.688 μmol/min*mg protein) using GPxA as redox partner [25]. However, we were unable to reproduce this previous result; when mixing the cytosolic-enriched fraction with recombinant GPxA, the assay mix precipitated. Nevertheless, GPxA replacement with TXNPx allowed consistent determination of the TXN activity, showing lower activity and therefore the lowest catalytic efficiency (*Vmax*/*Km*) in the parasites. To further ensure that the *Vmax* value of TXN was not underestimated, an assay was performed using increasing NADPH, TryR, $T(SH)_2$, TXNPx and CumOOH (Fig. S2B); the resulting TXN activity remained unchanged. Moreover, there was no activity displayed if any of the system components were omitted (Fig. S2A).

TXNPx and GPxA kinetics in soluble cell fraction were determined using the coupling systems TryR/$T(SH)_2$/TXN or GSH/GR, respectively, and CumOOH or t-butOOH (Fig. S7; Table 1). The peroxidase activity that was detected in the soluble fraction of the parasites using the TryR/$T(SH)_2$/TXN coupling system mainly corresponded to that of TXNPx because: (a) in the enzymatic assay, the hydroperoxide reduction activity was inactivated at high dilution of the cell sample (concentration <0.1 mg protein/ml) in a similar fashion to the behavior displayed by TXNPx recombinant enzyme (data not shown). Therefore, the TXNPx *Vmax* in the parasite reported in Table 1 was always determined at a cellular protein concentration greater than 0.2 mg/ml. (b) The peroxidase activity in the soluble fraction was inhibited at >100 μM CumOOH or t-butOOH like that of the recombinant enzyme; no other components that increased activity at higher peroxide concentrations (which could indicate GPxA activity) were observed (Fig. S7). And (c) a saturating behavior was observed at 100 μM of the peroxides (Fig. S7), which corresponded to 10-fold the Km_{app} *CumOOH* (or Km_{app} *t-butOOH*) of recombinant TXNPx, but only onefold (or less) the *Km* of GPxA (Table 1).

The *Km* and *Ki* values of TXNPx present in the parasite soluble fraction were also determined (Table 1). These values were similar to those of the recombinant enzyme which further supported that the main peroxidase activity in the parasite corresponded to TXNPx.

To search for GPxA activity in the cell soluble fraction, the GSH/GR coupling system was used since TXNPx is not able to interact with this other coupling system. A low activity was determined (Table 1); the value was recalculated assuming that in this coupling assay the recombinant GPxA displayed only 10% of its full activity. The GPxA value in the cells resulted to be 2.5 lower than that of TXNPx (Table 1).

3.3. Properties of the in vitro pathway reconstitution

Kinetic characterization of the recombinant enzymes allowed distinguishing the activity of each enzyme in the cell in order to reconstitute the pathway at physiological pH and temperature. The proportion of enzyme activities determined in the soluble cytosolic-enriched fraction of the parasites is shown in Table 2. For pathway reconstitution with the recombinant enzymes two TXN-dependent systems were separately analyzed: one constituted by TryR/$T(SH)_2$/TXN/TXNPx and another in which TXNPx is replaced by GPxA. It should be noted that a reconstituted system with the two peroxidase activities included would be disadvantageous for GPxA, as only short-chain hydroperoxides were used in these experiments and TXNPx has much lower Km_{app} for these substrates.

The appropriate range of enzyme activity (always maintaining the same ratio) to attain experimentally reliable changes in flux was first determined, considering the incubation time and spectrophotometer sensitivity. It turned out that 264 mU TryR: 88 mU TXN: 177 mU TXNPx were the most reliable and reproducible ratio activities for pathway reconstitution, which were similar to the activities determined in 1 mg of parasite cellular protein (Table 1). It is noted that 177 mU TXNPx corresponds to 14–18 μg protein/ml in the reconstitution experiments; this high concentration prevented its inactivation by dilution. Moreover, at the lowest percentage titrated value of TXNPx activity (25%, ~4 μg protein/ml), the enzyme was not yet inactivated.

To further explore the physiological validity of this *in vitro* reconstituted pathway with the recombinant enzymes, the flux of peroxide reduction attained with the native enzymes present in the parasite cytosolic-enriched fraction was determined. A linear dependency of reduction of H_2O_2 and CumOOH on the amount of protein was obtained, with values of 4.2 ± 0.8 (n = 3) and 3.0 ± 1.3 (n = 3) nmol/min* mg protein, respectively (Fig. 3). In the reference reconstituted pathway, which contains the same units of recombinant enzyme activities than those found in the cytosolic-enriched fractions, the CumOOH reduction flux was 4.9 ± 2.4 nmol/min (n = 5). This indicated that the reference reconstituted pathway was able to reproduce the flux attained by the enzymes present in the fraction of the parasites.

Molecular crowding seemed not to affect the pathway behavior. In the reference reconstituted pathway with the recombinant enzymes the total protein concentration was ~0.02 mg/ml, and the flux obtained was almost the same than that achieved with the cellular cytosolic fraction, where the maximum total protein amount reached in the assay was 5 mg/ml (Fig. 3). Furthermore, pathway reconstitution was carried out in the presence of various PEG 8000 and DMSO concentrations. Pathway flux rates were unaffected by 5–10% PEG 8000, whereas higher concentrations of both crowding agents were detrimental for the pathway flux (Table S2).

3.4. Flux control distribution

The C^J_{ai} of an enzyme/process belonging to a metabolic pathway is determined from the dependence of the pathway flux on variation in the activity of a single enzyme or group of enzymes [20,21]. Thus, the activity of TryR, TXN, TXNPx or GPxA was varied one at a time. The activity of each enzyme was varied above and below the point of interest (100% activity), which for the *in vitro* reconstituted system was the enzyme activity present in 1 mg protein of the parasite soluble fraction. The C^J_{ai} values were determined from the derivative at the point of interest (100% activity) from the curve of the global non-linear fitting of the experimental data (Fig. 4).

A requisite for proper MCA application is that the reconstituted pathway be under steady-state conditions regarding pathway flux and intermediary concentrations (*i.e.* the rate of pathway flux and the pathway metabolite concentrations have to be constant). A pseudo steady-state (because of net substrate consumption) pathway flux was obtained for at least two minutes after initiating the reaction with the peroxide (Fig. S8). During this time-period the $T(SH)_2$ concentration was maintained nearly constant, at ~90% of the initial value (Fig. S8). These results suggested that the reconstituted pathway was under steady-state which made it appropriate for C^J_{ai} determination

For the reconstituted pathway with TXNPx, titrations with TXN and TXNPx yielded a near-linear response in the flux to variations in their activities (Fig. 4B and C) each one rendered a C^J_{ai} close to 1 (Table 2).

Table 2
Flux control coefficients obtained by pathway reconstitution.

Enzyme	*In vivo* ratio	C^J_{ai}	
		with TXNPx	with GPxA
TryR	3	0.2 ± 0.04 (3)	0.2 (2)
TXN	1	1 ± 0.1 (3)	1.1 (2)
TXNPx	2	1 ± 0.1 (3)	
GPx	0.8		0.9 (2)

Values are mean ± SD. Numbers in parenthesis indicate the number of independent experiments assayed.

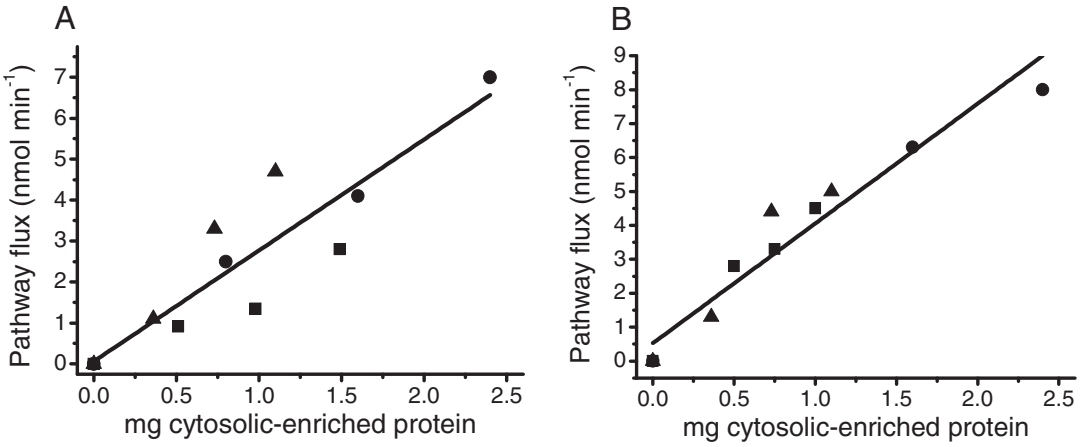

Fig. 3. Determination of the pathway flux in the parasite soluble cytosolic-enriched fraction. The fluxes of reduction of 0.1 mM CumOOH (A) and 30–100 μM H_2O_2 (B) were determined at saturating concentrations of NADPH and $T(SH)_2$ and different amounts of parasite protein obtained from different culture batches (indicated with different symbols). The flux rate corresponded to the slope of the linear fitting (solid lines).

In contrast, TryR showed a C^J_{ai} of 0.2 (Fig. 4A), indicating that this enzyme exerted a control of only 10% on the hydroperoxide reduction flux. The sum of the C^J_{ai} was near two, not one as occurs for linear metabolic pathways [20,21]. It has been demonstrated that in metabolic pathways in which there is transfer of groups (electrons or phosphates) such as in the mitochondrial respiratory chain, the sum of the control coefficient is higher than one [36–38].

For the reconstituted pathway with GPxA, again, variations in TXN and GPxA produced a linear response on the hydroperoxide reduction flux (Fig. 4E and F) and $C^J_{ai} = 1$ for each one (Table 2). This reference reconstituted pathway was performed using 10 fold GPxA because its activity was underestimated in the GSH/GR coupling assay. Despite these shortcomings, the C^J_{ai} did not change in the whole interval of titration. TryR activity was also in excess for this system and therefore showed a low C^J_{ai} (Fig. 4D; Table 2).

3.5. Apparent affinities of the tryparedoxin-dependent hydroperoxide detoxification pathway for different metabolites

For the above-described results, the reference reconstituted pathway with TXNPx used saturating concentrations of NADPH, $T(SH)_2$ and CumOOH (according to the *Km* values of the individual enzymes); however, the Km_{app} values of the complete pathway may be different to those of the individual enzymes since new kinetic properties emerge when the complete pathway is analyzed [19]. Therefore, the kinetic behavior of the whole pathway to variation in the substrate concentration was determined (Fig. 5). These pathway Km_{app} values are described in Table 3.

The $Km_{app\ CumOOH}$ of the whole system did not vary in comparison to the Km_{app} values of TXNPx for several peroxides (Table 1); substrate inhibition was also observed in the reconstituted system (Fig. 5). However, the whole system showed higher Km_{app} than TryR for NADPH and lower Km_{app} than TXN for $T(SH)_2$. For the first observation, it is possible that TS_2 generated by the system does not saturate TryR leading to higher *Km* values for co-substrates; an explanation for the second observation may be that a higher degree of enzyme coupling in the reconstituted system leads to lower *Km* values for substrates. This suggests that other controlling/regulatory interactions in the pathway are taking place when the enzymes are working together in the whole pathway; thus, the enzyme rates will depend on the interactions with the other components of the system. By comparing the degrees of pathway saturation with some reported concentrations of NADPH and $T(SH)_2$ in the parasites, the system seemed partially limited by NADPH in comparison to $T(SH)_2$, which is in excess.

4. Discussion

The uniqueness of the TXN-dependent peroxide reduction pathway in *T. cruzi* has prompted the notion that drugs that may target its enzymes would be an adequate alternative strategy for therapy [7]. Gene essentiality has been applied for drug-target validation within this pathway [13–15] reviewed in [5,6,8]. However, when gene essentiality is experimentally analyzed, usually very high degrees of enzyme inhibition are required to be reached within the cell by chemical or genetic near-knockout. Under such conditions, it can be expected that any pathway enzyme indeed affects the pathway flux. On the other hand, comparison of the kinetic properties determined with pure enzymes is another qualitative criterion to make predictions about rate limitation in metabolic pathways and drug targeting. This type of analysis has the shortcoming that kinetic characterizations are usually performed under optimal conditions of enzyme activity, which generally do not consider physiological parameters such as enzyme activity or metabolite concentrations in the cell.

It is thus recognized that additional criteria are necessary for drug target validation [6,7,16,17]. Hence, it is here proposed to apply the criterion of metabolic relevance to drug-target prioritization in the TXN-dependent peroxide detoxification pathway. MCA provides a *quantitative* analysis on the degree of control of the enzymes over the pathway flux. This biochemical framework considers the enzymes/transporters as functional parts of a whole interacting system and not just as the sum of the properties of the individual entities [20–22]. That is the power of making systemic analysis of whole metabolic pathways to establish mechanisms of control. Computational modeling and MCA was recently applied to the $T(SH)_2$ synthesis pathway and identified γ-glutamylcysteine synthetase and TryS as the most controlling enzymes [25]. In the present study, MCA was applied to the TXN-dependent peroxide detoxification system.

4.1. Analysis of the kinetic properties of the enzymes in isolation and within the cell

It was previously suggested that the electron transfer from $T(SH)_2$ to TXN was the rate-limiting step of the pathway due to its low catalytic potential; however, the $kcat/Km_{app}$ ratios were determined at optimal pH (8.0) and 25 °C [33]. The kinetic properties of *T. cruzi* TryR, TXN, TXNPx and GPxA were all here re-evaluated ([25] and present study) under the same enzymatic assay conditions, which resembled the physiological intracellular pH and temperature at which the human infective stage of the parasite lives. Comparison of the $kcat/Km_{app}$ ratio values

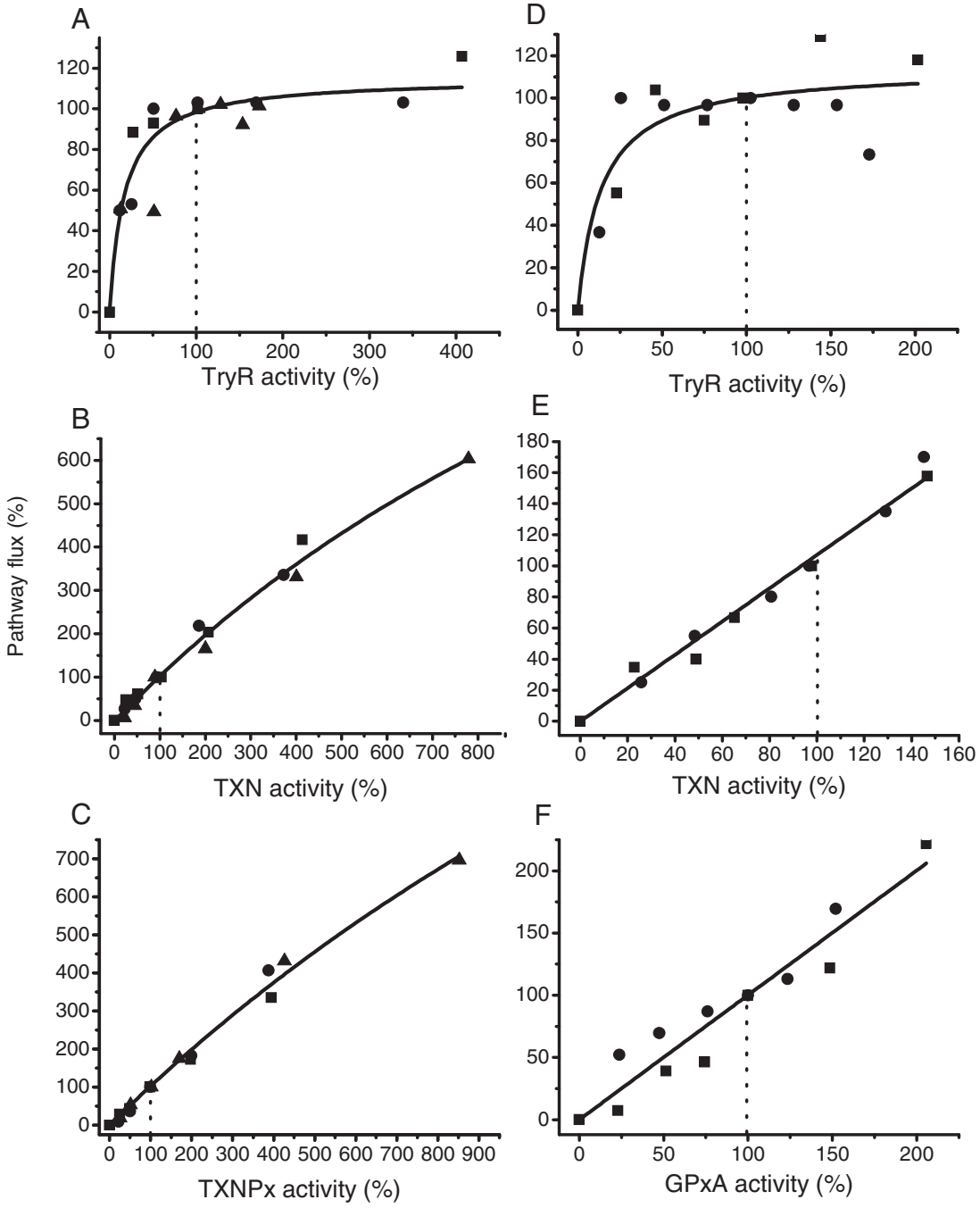

Fig. 4. Determination of the C^{J}_{ai} of the trypanothione-dependent detoxifying enzymes in an *in vitro* reconstituted pathway. Reconstituted pathway with TryR, TXN and either TXNPx (panels A, B, C) or GPxA (panels D, E, F). Each enzyme was independently varied above and below their activities determined in the soluble cytosolic fractions, which were 264 mU TryR, 88 mU TXN and 177 mU TXNPx or 70 mU GPxA. While varying one enzyme, the other enzymes were kept at the reference activity; saturating concentrations of NADPH (0.16 mM), $T(SH)_2$ (0.45 mM) and CumOOH (0.1 mM) were used. Each symbol represents a titration performed with a different enzyme batch. The solid lines represent global fittings to a hyperbola (without a mechanistic meaning), which was done using the Origin 8 software. The C^{J}_{ai} were determined from the derivative at the reference point of 100% activity and flux.

obtained under these conditions indeed showed that TXN reduction exhibited the lowest value (Table 1). However, a low $kcat/Km_{app}$ ratio of the isolated recombinant enzyme could be *in vivo* compensated by a high content of active enzyme in the cell.

In this regard, it has been determined that TXN accounts for up to 3% of the total protein content in *T. cruzi* epimastigotes, as calculated from the purification yield, and *kcat* and *Vmax* values [33]. In contrast, when using the TXN *kcat* and *Vmax* determined in the present work (Table 1) and the equation $Vmax = kcat\ x$ [total active enzyme], the TXN content in *T. cruzi* epimastigotes accounted for only 0.1% of the total protein. As Wilkinson et al. [33] kinetic characterization of the enzyme was carried out with sub-saturating concentrations of substrates and coupling enzymes (20 μM $T(SH)_2$ = 0.5-fold Km_{app}; 2 μM TcGPxA = 1-fold Km_{app}; 0.5 μM TryR = 0.5 fold vs. TXN protein content; 20 μM CumOOH = 1-fold Km_{app} for GPxA), the resulting underestimated *in vitro* *V*max and *kcat* values very likely led to overestimation of the percentage of protein in the cell. Our results indicated that in the cell, TXN has low *Vmax* and high *Km* for $T(SH)_2$, which imposes a rate limitation in the pathway flux.

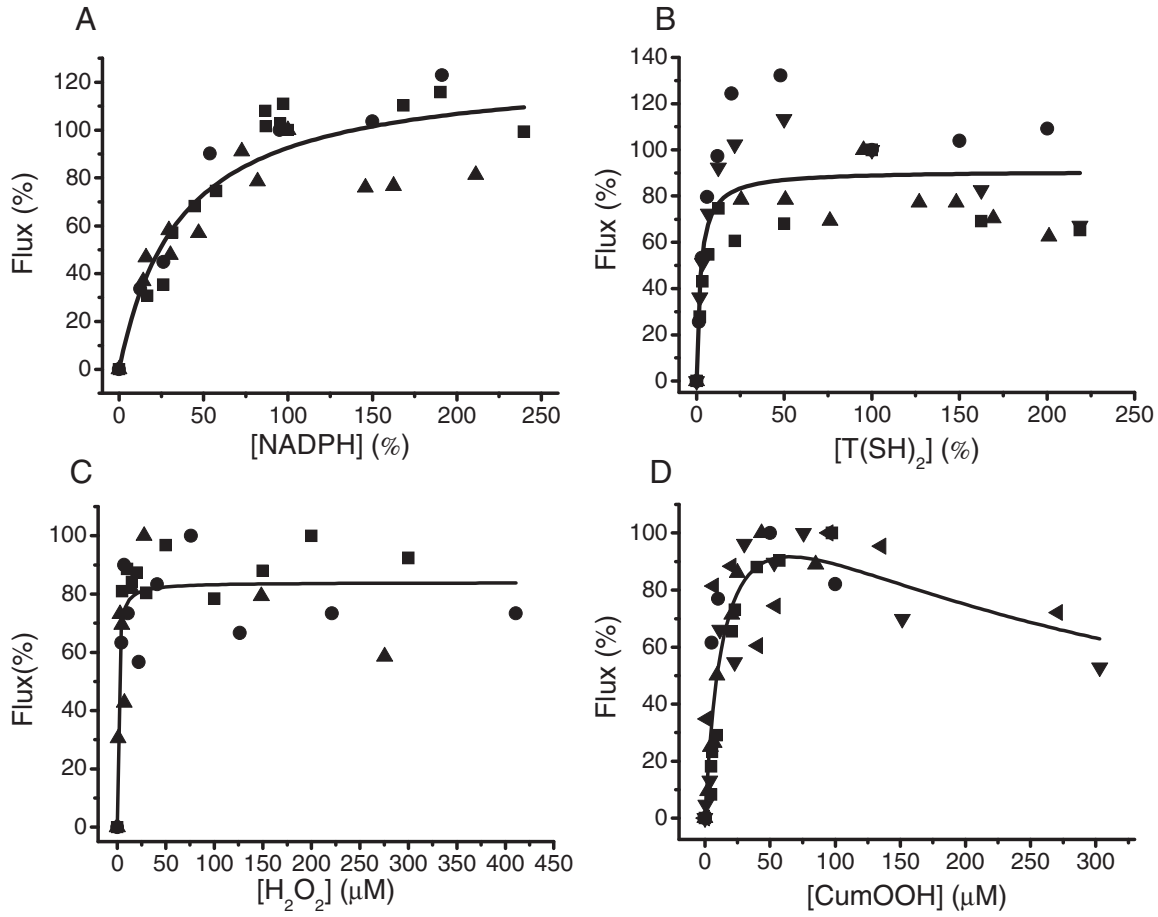

Fig. 5. Kinetics of the reconstituted TXN-dependent detoxification pathway using TXNPx. When one substrate was varied, the co-substrate concentrations were kept constant at the saturating values of 0.16 mM NADPH, 0.45 mM $T(SH)_2$ and 0.1 mM CumOOH. In (A) and (B) the pathway flux was normalized to the flux attained at the physiological concentration of 0.084 mM NADPH [25] and 0.3 mM $T(SH)_2$ [5], respectively. In (C) and (D), the flux was normalized to the maximum flux value obtained in each titration made with 0–0.45 mM [H_2O_2] or 0–0.3 mM [CumOOH]. Each symbol represents a titration performed with a different enzyme batch.

The present kinetic analysis identifies TXN as the less efficient pathway enzyme on the basis of its apparent low catalytic efficiency within the cell. However, the degree of saturation of the enzymes by the physiological concentrations of metabolites and the degree of coupling among the system components also affect the pathway flux and therefore require consideration as well. The *in vivo* flux of the entire metabolic pathway, and therefore of the partial rate of each pathway enzyme, will depend on the kinetic parameters, substrate concentrations and regulatory mechanisms of the four enzymes in the system [20–22]. It is worth recalling that under steady-state conditions, the rates of the individual steps of a metabolic pathway are the same and equal to the pathway flux, with the condition that the pathway is linear and there are no changes in metabolite stoichiometry [20,21]. Therefore, an integral analysis which includes all these parameters was accomplished by *in vitro* reconstitution of the pathway.

Table 3
Kinetic parameters of the complete reconstituted system.

Metabolite	$[Metabolite]_{physiological}$ (μM)	Km_{app} (μM)	$[metabolite]_{physiological}/Km_{app}$ ratio
NADPH	84[a]	37 ± 15 (3)	2.3
$T(SH)_2$	300[b]	2.7 ± 0.4 (4)	111
H_2O_2	0.01–10	0.9 ± 0.4 (3)	0.01–11.1
CumOOH		16 ± 6 (5)	0.0006–0.6

Reported physiological metabolite concentration [a] [25], [b] [39].

4.2. Flux control distribution of the TXN-dependent peroxide detoxification system

In vitro reconstitution of metabolic pathways is a MCA strategy that has been previously applied to determine the C^J_{ai} for some sections of glycolysis in mammalian cells [40,41] and the human parasite *Entamoeba histolytica* [42]. The controlling steps identified by this strategy have been in agreement with metabolic modeling of glycolysis in normal cells [43,44], tumor cells [45] and *E. histolytica* [46]. Therefore, MCA of the peroxide detoxification pathway can provide insight into the mechanisms of control of the pathway.

The flux rates of the reconstituted TXN-dependent hydroperoxide detoxification pathway with the recombinant enzymes were similar to those attained by the fraction of the parasites, validating the *in vitro* system used. The prevalent $T(SH)_2$ pathway in the parasite is cytosolic [8,33,34]; therefore, it was considered that the enzyme kinetic and controlling behavior would be representative of that of the pathway in the cytosol. Thus, the *in vitro* simplification of a section of the complex antioxidant machinery in *T. cruzi* can be used to identify the main controlling pathway reactions. The direct quantitative determination of the flux control distribution in intact cells certainly provides a more rigorous approach, than *in vitro* pathway reconstitution, for the identification of suitable drug targets. However, the specificity of peroxide reduction by the TXN-dependent pathway using living cells may not be ensured because of the background caused by unspecific reactions of the peroxides with the incubation medium, the high content of intracellular

antioxidants such as GSH and $T(SH)_2$ and the activity of other peroxidases not dependent on TXN. Moreover, quantitative strategies to determine dynamic intracellular ROS concentrations are currently limited because of the irreversible oxidation of the fluorescent dyes used for such experiments [47].

Our results indicated that the TXN–TXNPx and TXN–GPxA redox pairs have total control on the hydroperoxide reduction system with remarkably low control by TryR. The sum of the C^J_{ai} was higher than 2, apparently contradicting the summation theorem of MCA which states that the sum of the positive and negatives C^J_{ai} of the enzymes of a metabolic pathway should be 1 [20–22]. This issue has been theoretically analyzed for group-transfer pathways in which the sum of $C^J_{ai} \approx 2$ has been found [36,37,48]. It has also been experimentally tested for the flux control distribution of the mitochondrial respiratory electron transfer chain [38], and activation/deactivation in signaling pathways by phosphorylation/dephosphorylation [49]. The mechanistic explanation is that, contrary to what occurs in typical metabolic pathways where the substrates and products of the enzymes are released to the medium, in group-transfer pathways the enzymes transfer the groups hand-to-hand; hence, each enzyme is involved simultaneously in two reactions (*e.g.* oxidation and reduction; phosphorylation and dephosphorylation), and the pathway is organized in channeling. That is the reason why the sum of the C^J_{ai} is two when enzyme titration is the method to determine the flux control distribution [37].

The degree of coupling between TXN and the peroxidases due to the internal organization of the metabolic pathway indicated that interruption of one of the electron transfer components, TXN, and TXNPx or GPxA, will completely halt the pathway flux. In fact, the *in vivo* TXN interactome has suggested that there could be structural interaction between TXN and TXNPx [50].

Therefore, based on this metabolic quantitative analysis it is proposed that the most convenient drug target in the TXN-dependent hydroperoxide reduction pathway is TXN. This dithiol protein has high control on the flux and its inhibition will affect the two peroxide detoxification branches. In this regard, inhibitors have been identified by high-throughput screening that target *T. brucei* TXN [51]. In contrast, decreasing the peroxide reduction capacity by inhibiting TryR appears to be a more challenging task due to its low control on the flux of peroxide reduction (present study) and $T(SH)_2$ synthesis [25]. TryR can have important homeostatic control on the $T(SH)_2$/TS_2 concentration ratio (in a similar way to that of adenylate kinase in maintaining the balance of the adenine nucleotides in the cells). However, since parasite cells seem to have a high concentration of the $T(SH)_2$ moiety, the high activity and catalytic efficiency of TryR provide overcapacity in recycling the $T(SH)_2$ for the peroxide reduction system flux. Therefore, much higher levels of TryR inhibition (i.e. chemical or genetic knockout), than that of TXN, appear mandatory to be able to affect the hydroperoxide reduction capabilities of the parasites.

4.3. Reductive power may limit the peroxide reduction flux under high oxidative stress

The difference in the kinetic parameters of the whole system in comparison to those of the isolated enzymes indicated that additional regulatory factors emerge when the enzymes work together in the whole system, that ultimately determine the pathway flux. The analysis suggested that at low concentrations, peroxide supply will determine the pathway flux whereas at high concentrations, the physiological NADPH supply may be limiting. In turn, the $T(SH)_2$ concentration used here corresponds to one of the lowest reported values [39]; however, other concentrations have been determined (0.06–7 mM) which depend on the parasite stage, phase of growth as well as the degree of oxidative stress [8,25].

5. Conclusion

MCA applied to the TXN-dependent hydroperoxide detoxification system in *T. cruzi* was able to quantitatively prioritize drug-targets in the pathway. The redox-pairs TXN-peroxidases were identified as the most flux-controlling pathway enzymes. Since TXN is at the crossroad of the two main peroxide detoxification mechanisms in the cell, it is herewith proposed that TXN is a more suitable candidate for drug targeting. Although the approach used here has the inconvenience of being an *in vitro* experimental model, the pathway organization in the cell might be similar to the one attained *in vitro*.

Due to the organizational similarities of the TXN-dependent hydroperoxide detoxification pathway in the main three trypanosomatid species, similar flux control distribution of the TXN redox pairs can be expected. Hence, the results found here using the *in vivo* parameters determined in the epimastigote stage of *T. cruzi*, should lead to focus drug therapy research of trypanosomiasis on using TXN as target in the *T. cruzi* trypomastigotes and in other trypanosomatids.

Acknowledgments

This work received financial support from CONACyT Mexico grant no. 178638 to ES. ZG-Ch received financial support from CONACyT fellowship no. 392956; he also acknowledges partial support to Programa de Maestría y Doctorado en Ciencias Bioquímicas de la UNAM. We thank to I. García-Cano, Citlali Vázquez and Aketzalli Silva for the technical assistance.

Appendix A. Supplementary data

Supplementary data to this article can be found online at http://dx.doi.org/10.1016/j.bbagen.2014.10.029.

References

[1] J.R. Coura, J. Borges-Pereira, Chagas disease. What is known and what should be improved: a systemic review, Rev. Soc. Bras. Med. Trop. 45 (3) (2012) 286–296.
[2] J.D. Maya, M. Orellana, J. Ferreira, U. Kemmerling, R. López-Muñoz, A. Morello, Chagas disease: present status of pathogenic mechanisms and chemotherapy, Biol. Res. 43 (3) (2010) 323–331.
[3] D. Spinks, E.J. Shanks, L.A. Cleghorn, S. McElroy, D. Jones, D. James, A.H. Fairlamb, J.A. Frearson, P.G. Wyatt, I.H. Gilbert, Investigation of trypanothione reductase as a drug target in *Trypanosoma brucei*, ChemMedChem 4 (12) (2009) 2060–2069.
[4] S.R. Wilkinson, J.M. Kelly, The role of glutathione peroxidases in trypanosomatids, Biol. Chem. 384 (4) (2003) 517–525.
[5] R.L. Krauth-Siegel, M.A. Comini, Redox control in trypanosomatids, parasitic protozoa with trypanothione-based thiol metabolism, Biochim. Biophys. Acta 1780 (11) (2008) 1236–1248.
[6] V. Olin-Sandoval, R. Moreno-Sánchez, E. Saavedra, Targeting trypanothione metabolism in trypanosomatid human parasites, Curr. Drug Targets 11 (12) (2010) 1614–1630.
[7] L. Flohé, The trypanothione system and the opportunities it offers to create drugs for the neglected kinetoplast diseases, Biotechnol. Adv. 30 (1) (2012) 294–301.
[8] F. Irigoín, L. Cibilis, M.A. Comini, S.R. Wilkinson, L. Flohé, R. Radi, Insights into the redox biology of *Trypanosoma cruzi*: trypanothione metabolism and oxidant detoxification, Free Radic. Biol. Med. 45 (6) (2008) 733–742.
[9] M.D. Piñeyro, A. Parodi-Talice, T. Arcari, C. Robello, Peroxiredoxins from *Trypanosoma cruzi*: virulence factors and drug targets for treatment of Chagas disease? Gene 408 (1–2) (2008) 45–50.
[10] L. Piacenza, M.P. Zago, G. Peluffo, M.N. Alvarez, M.A. Basombrio, R. Radi, Enzymes of the antioxidant network as novel determiners of *Trypanosoma cruzi* virulence, Int. J. Parasitol. 39 (13) (2009) 1455–1464.
[11] D.G. Arias, V.E. Marquez, M.L. Chiribao, F.R. Gadelha, C. Robello, A.A. Iglesias, S.A. Guerrero, Redox metabolism in *Trypanosoma cruzi*: functional characterization of tryparedoxins revisited, Free Radic. Biol. Med. 63 (2013) 65–77.
[12] M. Diechtierow, R.L. Krauth-Siegel, A tryparedoxin-dependent peroxidase protects African trypanosomes from membrane damage, Free Radic. Biol. Med. 51 (4) (2011) 856–868.
[13] S. Krieger, W. Schwarz, M.R. Ariyanayagam, A.H. Fairlamb, R.L. Krauth-Siegel, C. Clayton, Trypanosomes lacking trypanothione reductase are avirulent and show increased sensitivity to oxidative stress, Mol. Microbiol. 35 (3) (2000) 542–552.
[14] M.A. Comini, R.L. Krauth-Siegel, L. Flohé, Depletion of the thioredoxin homologue tryparedoxin impairs antioxidative defence in African trypanosomes, Biochem. J. 402 (1) (2007) 43–49.

[15] S.R. Wilkinson, D. Horn, S.R. Prathalingam, J.M. Kelly, RNA interference identifies two hydroperoxide metabolizing enzymes that are essential to the bloodstream form of the African trypanosome, J. Biol. Chem. 278 (34) (2003) 31640–31646.
[16] L. Flohé, The trypanothione system and its implications in the therapy of trypanosomatid diseases, Int. J. Med. Microbiol. 302 (4–5) (2012) 216–220.
[17] R.L. Krauth-Siegel, A.E. Leroux, Low molecular-mass antioxidants in parasites, Antioxid. Redox Signal. 17 (4) (2012) 583–607.
[18] J.J. Hornberg, F.J. Bruggeman, B.M. Bakker, H.V. Westerhoff, Metabolic control analysis to identify optimal drug targets, Prog. Drug Res. 64 (2007) 171,173–171,189.
[19] A. Kolodkin, F.C. Boogerd, N. Plant, F.J. Bruggeman, V. Goncharuk, J. Lunshof, R. Moreno-Sanchez, N. Yilmaz, B.M. Bakker, J.L. Snoep, R. Balling, H.V. Westerhoff, Emergence of the silicon human and network targeting drugs, Eur. J. Pharm. Sci. 46 (4) (2012) 190–197.
[20] R. Moreno-Sánchez, E. Saavedra, S. Rodríguez-Enríquez, V. Olín-Sandoval, Metabolic control analysis: a tool for designing strategies to manipulate metabolic pathways, J. Biomed. Biotechnol. 2008 (2008) 597913.
[21] D. Fell, Understanding the Control of Metabolism, Portland Press, London, 1997.
[22] H.V. Westerhoff, Signalling control strength, J. Theor. Biol. 252 (3) (2008) 555–567.
[23] V. López-Olmos, N. Pérez-Nasser, D. Piñero, E. Ortega, R. Hernandez, B. Espinoza, Biological characterization and genetic diversity of Mexican isolates of *Trypanosoma cruzi*, Acta Trop. 69 (1998) 239–254.
[24] J.F. Fernandes, O. Castellani, Growth characteristics and chemical composition of *Trypanosoma cruzi*, Exp. Parasitol. 18 (2) (1966) 195–202.
[25] V. Olin-Sandoval, Z. González-Chávez, M. Berzunza-Cruz, I. Martínez, R. Jasso-Chávez, I. Becker, B. Espinoza, R. Moreno-Sánchez, E. Saavedra, Drug target validation of the trypanothione pathway enzymes through metabolic modelling, FEBS J. 279 (10) (2012) 1811–1833.
[26] M.A. Comini, N. Dirdjaja, M. Kaschel, R.L. Krauth-Siegel, Preparative enzymatic synthesis of trypanothione and trypanothione analogues, Int. J. Parasitol. 39 (10) (2009) 1059–1062.
[27] D.U. Gommel, E. Nogoceke, M. Morr, M. Kiess, H.M. Kalisz, L. Flohé, Catalytic characteristics of tryparedoxin, Eur. J. Biochem. 248 (3) (1997) 913–918.
[28] L. Flohé, P. Steinert, J.H. Hecht, B. Hofmann, Tryparedoxin and tryparedoxin peroxidase, Methods Enzymol. 347 (2002) 244–258.
[29] S.A. Guerrero, J.A. Lopez, P. Steinert, M. Montemartini, H.M. Kalisz, W. Colli, M. Singh, M.J. Alves, L. Flohé, His-tagged tryparedoxin peroxidase of *Trypanosoma cruzi* as a tool for drug screening, Appl. Microbiol. Biotechnol. 53 (4) (2000) 410–414.
[30] S.R. Wilkinson, D.J. Meyer, J.M. Kelly, Biochemical characterization of a trypanosome enzyme with a glutathione-dependent peroxidase activity, Biochem. J. 352 (Pt 3) (2000) 755–761.
[31] N. Van Der Heyden, R. Docampo, Intracellular pH in mammalian stages of *Trypanosoma cruzi* is K+-dependent and regulated by H+-ATPases, Mol. Biochem. Parasitol. 105 (2) (2000) 237–251.
[32] R.L. Krauth-Siegel, B. Enders, G.B. Henderson, A.H. Fairlamb, R.H. Schirmer, Trypanothione reductase from *Trypanosoma cruzi*. Purification and characterization of the crystalline enzyme, Eur. J. Biochem. 164 (1) (1987) 123–128.
[33] S.R. Wilkinson, D.J. Meyer, M.C. Taylor, E.V. Bromley, M.A. Miles, J.M. Kelly, The *Trypanosoma cruzi* enzyme TcGPXI is a glycosomal peroxidase and can be linked to trypanothione reduction by glutathione or tryparedoxin, J. Biol. Chem. 277 (19) (2002) 17062–17071.
[34] S.R. Wilkinson, N.J. Temperton, A. Mondragon, J.M. Kelly, Distinct mitochondrial and cytosolic enzymes mediate trypanothione-dependent peroxide metabolism in *Trypanosoma cruzi*, J. Biol. Chem. 275 (11) (2000) 8220–8225.
[35] O. Misset, O.J. Bos, F.R. Opperdoes, Glycolytic enzymes of *Trypanosoma brucei*. Simultaneous purification, intraglycosomal concentrations and physical properties, Eur. J. Biochem. 157 (2) (1986) 441–453.
[36] K. van Dam, J. van der Vlag, B.N. Kholodenko, H.V. Westerhoff, The sum of the control coefficients of all enzymes on the flux through a group-transfer pathway can be as high as two, Eur. J. Biochem. 212 (3) (1993) 791–799.
[37] M.D. Brand, B.P. Vallis, A. Kesseler, The sum of the flux control coefficients in the electron-transport chain of mitochondria, Eur. J. Biochem. 226 (3) (1994) 819–829.
[38] C. Bianchi, M.L. Genova, G. Parenti Castelli, G. Lenaz, The mitochondrial respiratory chain is partially organized in a supercomplex assembly: kinetic evidence using flux control analysis, J. Biol. Chem. 279 (35) (2004) 36562–36569.
[39] M.R. Ariyanayagam, A.H. Fairlamb, Ovothiol and trypanothione as antioxidants in trypanosomatids, Mol. Biochem. Parasitol. 115 (2) (2001) 189–198.
[40] N.V. Torres, F. Mateo, E. Meléndez-Hevia, H. Kacser, Kinetics of metabolic pathways. A system in vitro to study the control of flux, Biochem. J. 234 (1) (1986) 169–174.
[41] C. Giersch, Determining elasticities from multiple measurements of flux rates and metabolite concentrations. Application of the multiple modulation method to a reconstituted pathway, Eur. J. Biochem. 227 (1–2) (1995) 194–201.
[42] R. Moreno-Sánchez, R. Encalada, A. Marín-Hernández, E. Saavedra, Experimental validation of metabolic pathway modeling, FEBS J. 275 (13) (2008) 3454–3469.
[43] J. Puigjaner, B. Raïs, M. Burgos, B. Comin, J. Ovádi, M. Cascante, Comparison of control analysis data using different approaches: modelling and experiments with muscle extract, FEBS Lett. 418 (1–2) (1997) 47–52.
[44] F. Orosz, G. Wägner, F. Ortega, M. Cascante, J. Ovádi, Glucose conversion by multiple pathways in brain extract: theoretical and experimental analysis, Biochem. Biophys. Res. Commun. 309 (4) (2003) 792–797.
[45] A. Marín-Hernández, J.C. Gallardo-Pérez, S. Rodríguez-Enríquez, R. Encalada, R. Moreno-Sánchez, E. Saavedra, Modeling cancer glycolysis, Biochim. Biophys. Acta 1807 (6) (2011) 755–767.
[46] E. Saavedra, A. Marín-Hernández, R. Encalada, A. Olivos, G. Mendoza-Hernández, R. Moreno-Sánchez, Kinetic modeling can describe in vivo glycolysis in *Entamoeba histolytica*, FEBS J. 274 (18) (2007) 4922–4940.
[47] A. Hernández-Barrera, C. Quinto, E.A. Johnson, H.M. Wu, A.Y. Cheung, L. Cárdenas, Using hyper as a molecular probe to visualize hydrogen peroxide in living plant cells: a method with virtually unlimited potential in plant biology, Methods Enzymol. 527 (2013) 275–290.
[48] B.N. Kholodenko, H.V. Westerhoff, Metabolic channelling and control of the flux, FEBS Lett. 320 (1) (1993) 71–74.
[49] B.N. Kholodenko, J.M. Rohwer, M. Cascante, H.V. Westerhoff, Subtleties in control by metabolic channelling and enzyme organization, Mol. Cell. Biochem. 184 (1-2) (Jul 1998) 311–320.
[50] M.D. Piñeyro, A. Parodi-Talice, M. Portela, D.G. Arias, S.A. Guerrero, C. Robello, Molecular characterization and interactome analysis of *Trypanosoma cruzi* tryparedoxin 1, J. Proteomics 74 (9) (2011) 1683–1692.
[51] F. Fueller, B. Jehle, K. Putzker, J.D. Lewis, R.L. Krauth-Siegel, High throughput screening against the peroxidase cascade of African trypanosomes identifies antiparasitic compounds that inactivate tryparedoxin, J. Biol. Chem. 287 (12) (2012) 8792–8802.